LOW CYCLE FATIGUE PROPERTIES OF LPM™ WIDE-GAP REPAIRS IN INCONEL 738

Keith A. Ellison, Joseph Liburdi and Jan T. Stover†

Liburdi Engineering Limited, Hamilton, ON, Canada, L9J 1E7
†Consulting Engineer, Greenville, SC, 29611

Abstract

Strain controlled, continuous cycling and 2 minute compressive dwell LCF tests were performed on simulated LPM™ wide-gap repair joints in the nickel-base superalloy Inconel 738 at 850°C over a total strain range ($\Delta\epsilon_T$) of 0.4 to 0.9 percent, 0.33 Hz, A = ∞, R= -1. The test specimens were uncoated hybrid bars fabricated with a gauge section consisting of a cast inner core and an equal cross-sectional area overlayer of Inconel 738 LPM™ repair material. For samples with near-surface porosity of 0.25 mm and under, the fatigue lives of the LPM™ samples were about equal to those of cast Inconel 738 when $\Delta\epsilon_T < 0.5\%$, and approximately one-half to three-fourths for strains above this level. A two minute compressive hold reduced the fatigue lives of both the hybrid samples and cast Inconel 738 by a factor of 5 to 10 as compared to the continuous cycling tests, due to the increased creep, oxidation and mean-stress effects. In all cases, the dominant fatigue cracks initiated at near-surface pores. At strains below $\Delta\epsilon_T = 0.5\%$ crack propagation was transgranular, but shifted to an intergranular mode at higher strains. For specimens with near-surface porosity of approximately 0.5 mm, the fatigue lives were much shorter and initiation of the dominant cracks took place at these features. The results of these and other mechanical property tests indicate that, using the appropriate non-destructive inspection procedures and defect size restrictions, the LPM™ repair limits can potentially be extended into the more fatigue-sensitive areas of components such as airfoil leading edges.

Introduction

One of the most common types of service damage experienced by turbine hot section components is cracking due to thermal-mechanical fatigue. During a typical cycle of operation consisting of start-up, steady-state operation and shut-down, components experience a complex series of thermal and mechanical stresses. Under the most severe conditions, these stresses can cause local plastic deformation which, after a certain number of engine operating cycles, leads to thermal fatigue cracking. When the damage progresses beyond allowable limits, the components must be replaced or repaired.

Repair of cracked components has traditionally been carried out by fusion welding or diffusion brazing. Each process has its limitations. Weld repairs are often difficult and limited to lower-stressed areas of blades, such as airfoil tips and seal edges, due to their lower strength and susceptibility to heat affected zone cracks [1]. The quality of diffusion braze repairs is largely dependant on the efficiency of specialized hydrogen or hydrogen fluoride pre-cleaning processes which are used to remove corrosion products from the cracks. In practice, the effectiveness of the thermochemical cleaning processes has been reported to be inconsistent and the repairs are often ineffective. Poor thermal fatigue properties may result from incomplete crack cleaning, lack of filler metal penetration, the presence of pores and voids, brittle phase formation and cracking of the braze alloy itself [2,3].

The LPM™ wide-gap repair method was developed in order to overcome the limitations of both welding and diffusion brazing. Since LPM™ is capable of bridging gaps of 1 cm or more, defects can be mechanically removed, avoiding the potential pitfalls associated with special chemical cleaning operations mentioned above. The LPM™ filler material is comprised of superalloy powders in tape, slurry or putty form, with an overall composition (in the case of Inconel 738) similar to that of the base alloy. As a result, the mechanical properties approach those of the substrate material [4-6]. Finally, there are no problems related to restraint cracking or distortion since the material is fused and bonded in a vacuum heat treatment operation. This paper describes the results of laboratory low cycle fatigue (LCF) testing and field experience with LPM™ repairs in the nickel-base alloy Inconel 738.

Experimental Procedure

Tests were performed on simulated LPM™[1] wide-gap repair joints in the nickel-base superalloy Inconel 738. The LCF samples were hybrid specimens fabricated with a gauge section consisting of a cast inner core of Inconel 738 and an equal cross-sectional area overlayer of the Inconel 738 LPM™ repair material, Figure 1.

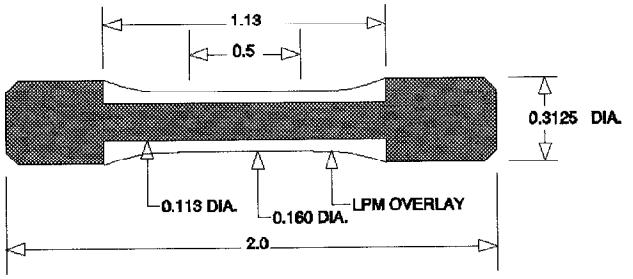

Figure 1. Sketch of the hybrid LPM™ overlay test specimen used to conduct the LCF tests.

[1] LPM™ (Liburdi Powder Metallurgy) is a patented and proprietary technology of Liburdi Engineering Limited.

Superalloys 1996
Edited by R. D. Kissinger, D. J. Deye, D. L. Anton,
A. D. Cetel, M. V. Nathal, T. M. Pollock, and D. A. Woodford
The Minerals, Metals & Materials Society, 1996

The cast Inconel 738 cores were machined from the root sections of scrap turbine buckets. These buckets had been previously HIP'ed to eliminate casting porosity which could otherwise lead to greater scatter in the mechanical properties. For these experiments, the LPM™ wide-gap filler material was applied in slurry form using a proprietary water-based binder. Due to the unusual joint geometry, it was necessary to apply and heat treat the LPM™ slurry in two or three operations by varying the specimen orientation for each cycle. This resulted in conditions, especially changes in the base alloy microstructure (see below) which were regarded as being more severe than those which would be encountered in a typical repair.

The compositions of the cast Inconel 738 LC and LPM™ wide-gap filler material are given in Table I.

Table I Composition of Inconel 738 Test Bars and LPM™ Wide-Gap Filler Alloy

Element	Nominal Composition (Weight Percent) Inconel 738LC	Inconel 738 LPM™
Ni	Balance	Balance
Cr	16	15.3
Co	8.5	9.0
Al	3.5	3.5
Ti	3.5	2.2
W	2.6	1.7
Ta	1.75	2.0
Mo	1.75	1.14
Cb	0.85	0.55
Zr	0.12	0.08
C	0.10	0.08
B	0.015	0.95

After application of the LPM™ filler material, the LCF specimens were processed through a vacuum heat treatment. The complete details of the cycle are proprietary, but in the case of Inconel 738 LPM™ repairs, processing is completed at a maximum temperature of 1200°C without any subsequent diffusion cycles. At this temperature, full solutioning of the cast Inconel 738 base alloy occurs, and consolidation and bonding of the LPM™ material takes place by liquid phase sintering. Primary aging of the LCF specimens was completed at 1120°C for 2 hours, followed by secondary aging at 843°C for 24 hours (i.e. the standard heat treatment for Inconel 738).

The bars were then rough machined to allow inspection by FPI and radiography. Removal of the final 0.40 mm of the gauge diameter on the LCF bars was accomplished by a low stress grinding procedure as described in ASTM E606-92, Section X3.

LCF testing was conducted according to ASTM E606-92 at Mar Test, Cincinnati, OH. Strain controlled, continuous cycling and hold time LCF tests were completed at 850°C over a total strain range of 0.4 to 0.9 percent. The continuous cycling tests were conducted at a frequency of 0.33 Hz, A=∞, R=-1. For the hold time tests, a two minute compressive dwell was added to each cycle. Load and strain outputs were plotted to produce total strain/time records as well as load/time records and periodic load/strain loops were generated during each test.

Cycles to crack initiation (N_i) was taken to be (a) the cycle on the alternating load vs. cycles plot at which the load decayed to approximately 90% of its initial stable level for a test in which the load decreased smoothly, or (b) the cycle at which a non-uniform change in character (slope) of the plot occurred, whichever was smaller. Cycles to failure (N_f) was taken to be the cycle at which the load dropped to below 30% of its initial stable value.

The effects of pore size and location on fatigue lives were studied by comparing the results of pre-test radiographic and penetrant inspections with visual, scanning electron microscope (SEM) and metallographic analyses of the fatigue crack origins.

Results

Low Cycle Fatigue Testing

The results of the continuous cycling and hold time tests are shown in Figures 2-4. Also shown are literature data for the cast Inconel 738 alloy. The literature data came from several sources, including the European COST 50 project and GE M&P Laboratory [7-9]. Nine samples were tested in the continuous cycling mode and three were used in the two-minute hold-time tests. Of these, two samples (one from each type of test) had much shorter lives than the others and were treated as outliers. It was later discovered that these two samples had larger porosity which was not typical of the rest of the specimens, as described below. All of the samples failed either within the gauge section or within the uniform section of the bar.

A plot of total strain range vs. cycles to crack initiation is shown in Figure 2. When represented in this form, the fatigue lives of the Inconel 738 LPM™ samples were approximately one-half those of cast Inconel 738 for $\Delta\epsilon_T \geq 0.5\%$, and about equal for strains below this level. The two minute compressive hold reduced the fatigue lives of the LPM™ samples by a factor of 5 to 10 as compared to the continuous cycling tests. As shown by the referenced data, a similar reduction in life is experienced by cast Inconel 738 alloy under these conditions. The difference in life between these test types (continuous cycling vs. 2 min. compressive hold) increases at lower strains for both materials.

For the continuous cycling tests, constants in the fatigue life relationship

$$\Delta\epsilon_T = AN_i^a + BN_i^b \quad (1)$$

where

$$\Delta\epsilon_e = \textit{elastic strain} = AN_i^a \quad (2)$$

and

$$\Delta\epsilon_p = \textit{inelastic strain} = BN_i^b \quad (3)$$

were determined by regression analysis, Figure 3. Over the range of the data, both $\Delta\epsilon_e$ and $\Delta\epsilon_p$ gave reasonable fits to the classical power law relationships. The four material constants were A = 1.024, a = -0.102 (correlation coefficient = -0.957); B = 3.841, b = -0.569 (correlation coefficient = -0.987).

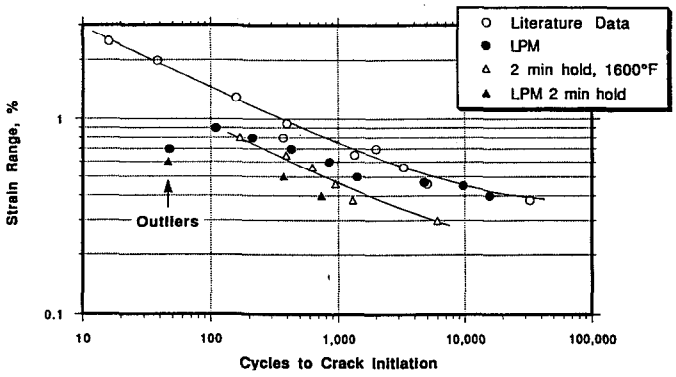

Figure 2. Plot of cycles to crack initiation vs. total strain range for LPM™ hybrid overlay samples compared against literature data for cast Inconel 738 alloy.

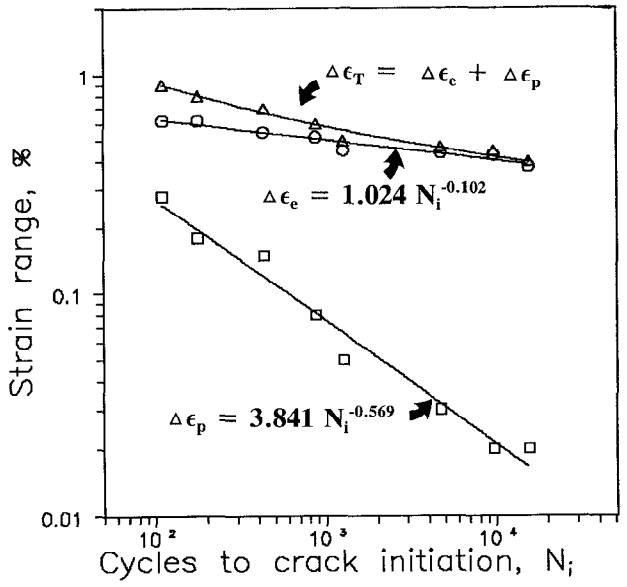

Figure 3. Fatigue life of the hybrid Inconel 738 overlay specimens on the basis of inelastic, elastic and total strain.

A plot of the inelastic strain range vs. cycles to crack initiation is shown in Figure 4. The inelastic strain range was determined near the half life of each sample by subtracting the elastic strain (calculated from the measured modulus of elasticity) from the total strain output by the machine control. For the two cases in which $N_i/N_f < 0.5$, the plastic strain was measured just prior to cycle N_i. For the remainder of the samples, the cyclic stress-strain response was approximately stable throughout 70 to 90 percent of the tests. When represented in this form, the fatigue lives of the Inconel 738 LPM™ samples were approximately three-fourths those of cast Inconel 738 for the higher strains, and again about equal for the lower strains.

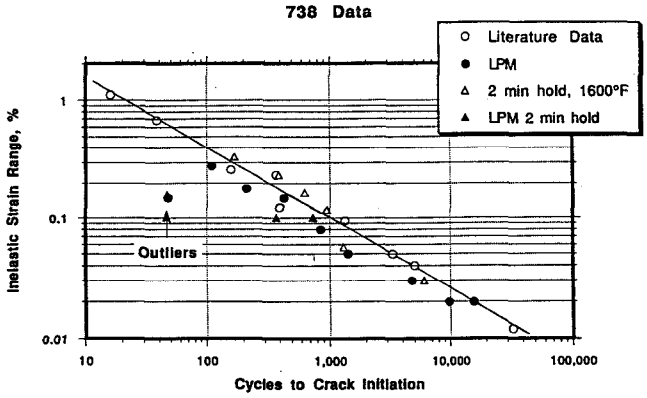

Figure 4. Plot of cycles to crack initiation vs. inelastic strain range for LPM™ hybrid overlay samples compared against literature data for cast Inconel 738 alloy.

A cyclic stress-strain plot for the triangular wave-form tests is shown in Figure 5. The stabilized stress values were determined at approximately 50% of fatigue life. A curve for the cyclic stress-strain data was fit using the Holloman relation:

$$\Delta\sigma/2 = k(\Delta\epsilon_p/2)^{n'} \quad (4)$$

A slight cyclic softening effect was observed which was quantified using the following expression:

$$\textit{Degree of hardening}(\%) = \frac{\Delta\sigma(\textit{half life}) - \Delta\sigma(\textit{start})}{\Delta\sigma(\textit{half life})} x100 \quad (5)$$

For the continuous cycling tests, the degree of softening was less than three percent. In contrast, the degree of softening in the trapezoidal, two minute compressive hold tests was much greater, at 3 to 15 percent. The increased effects of time-dependant damage (creep & oxidation) and the mean stresses generated in these tests were believed to be the major causes for the increased softening and reduced cycles to crack initiation [8].

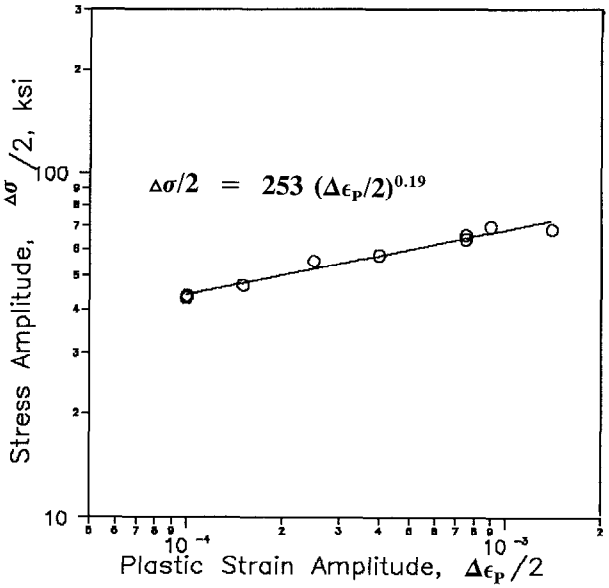

Figure 5 Cyclic stress-strain plot for Inconel 738 LPM™hybrid overlay specimens at 850°C.

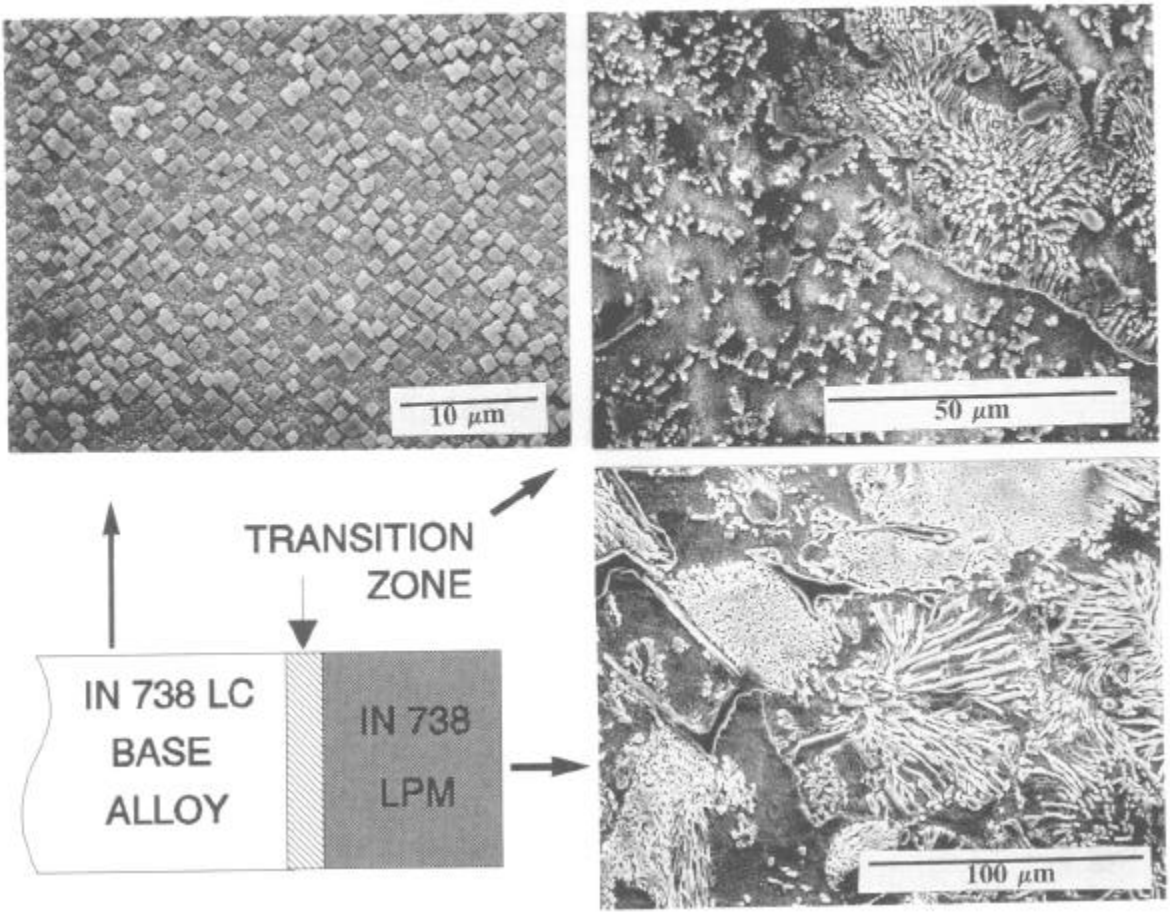

Figure 6. Schematic cross section of an LPM™ repair in Inconel 738 showing three microstructural zones: (1) an outer layer of LPM™ filler material, (2) a transition or diffusion zone and (3) the unaffected base alloy. The SEM images show typical microstructures within each zone.

Metallurgical Examination

Initial Structures. A schematic representation of a typical LPM™ repair is shown in Figure 6, which can be divided into three microstructural zones: (1) an outer layer of LPM™ filler material, (2) a transition or diffusion zone and (3) the unaffected base alloy. The Inconel 738 LPM™ filler microstructure consists of a uniform distribution of spherical gamma prime precipitates embedded in an austenitic gamma matrix. Scattered throughout this structure are eutectic gamma prime colonies, carbides, pores and irregular-shaped boride intermetallics. Previous tests have shown that the intermetallics, which form predominantly along the grain boundaries, are chromium-rich with minor amounts of tungsten and molybdenum and have a Cr_5B_3 structure.

The cast Inconel 738 base alloy contains a duplex gamma prime microstructure consisting of cuboidal primary and spherical secondary particles. The structure also contains large, randomly distributed MC carbides and $M_{23}C_6$ grain boundary carbides.

Within the diffusion zone, a gradual transition of structures is observed. Moving towards the base alloy, the number density of primary cuboidal gamma prime precipitates increases, while the volume fraction of eutectic gamma prime colonies and boride precipitates decreases. The depth of the diffusion zone typically lies between 0.25 to 0.50 mm. However, as noted earlier, the LPM™ filler was applied and heat treated in two or three build-ups. For this reason and also because of the fact that diffusion took place from all directions, the core of some of the hybrid LCF specimens was composed almost entirely of the transition structure. Consequently, the microstructure and properties determined in these tests are considered to represent a severe or worst case test of the LPM™ material.

Analysis of Fracture Surfaces. Low power optical examination and SEM imaging revealed that the dominant fatigue cracks initiated at near-surface pores in all of the LCF specimens. This was as expected, since LCF failures are generally associated with surface-related defects or discontinuities. However, metallographic sections revealed that the majority of pores, even those at the surface, were less than 0.25 mm in diameter and had not initiated fatigue cracks. The dominant fatigue cracks initiated at isolated larger pores located within approximately one pore diameter of the surface. In addition to the dominant crack, numerous secondary initiation sites were observed along the gauge section of each specimen. In general, there were more crack initiation sites at the higher strain ranges.

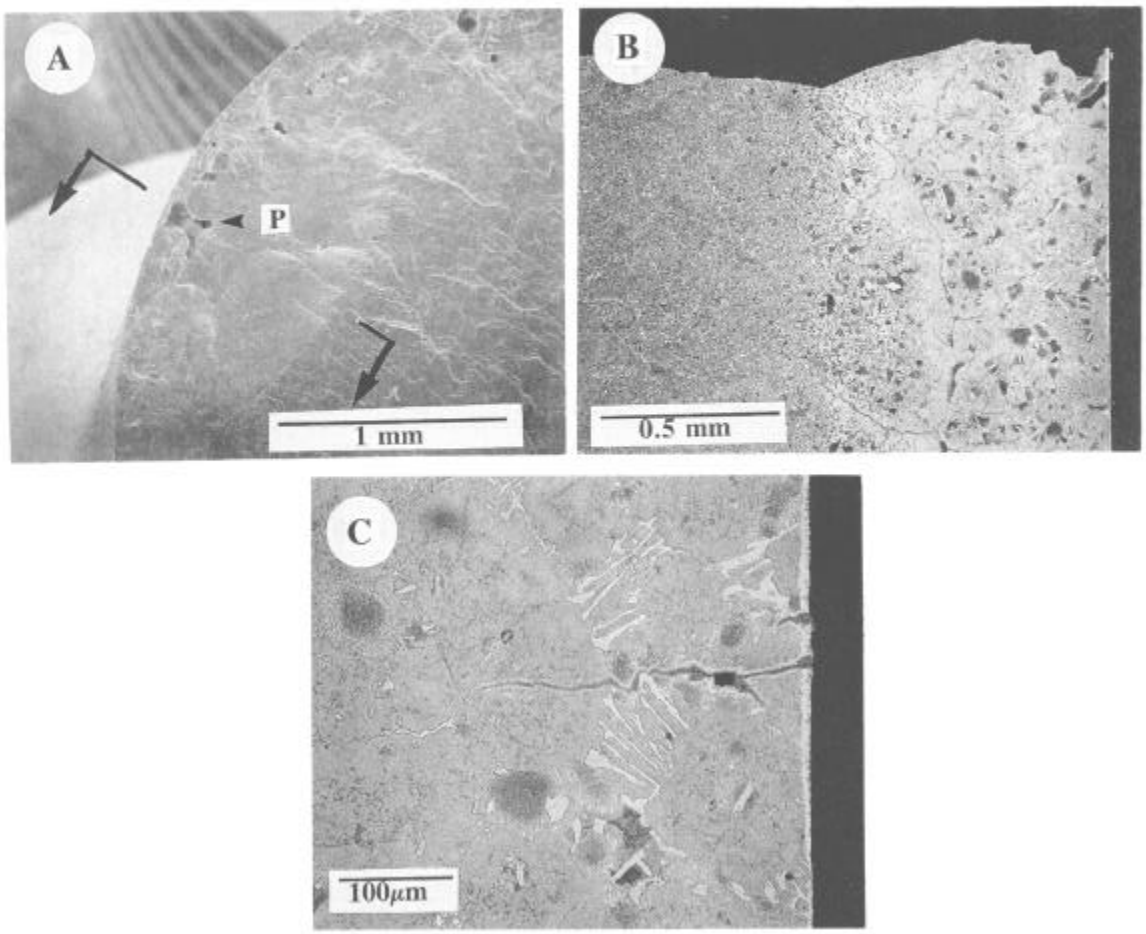

Figure 7. SEM fractograph (A) and optical micrographs (B,C) of the fatigue fracture surface on sample B13 ($\Delta\epsilon_T$ = 0.47%, N_f = 4741 cy., triangular wave form). The initiation site was a 0.18 mm x 0.18 mm pore (P) just beneath the surface of the uniform section. Arrows in (A) indicate the orientation of the metallographic section. This sample is representative of those tested with $\Delta\epsilon_T$ < 0.5% which had smooth fracture surfaces and transgranular crack propagation.

The fracture surfaces of the samples tested at strain ranges below $\Delta\epsilon_T$ = 0.5% were macroscopically smooth, with Stage II crack propagation taking place normal to the loading axis, Figure 7. Metallographic examination of the dominant and secondary cracks showed that propagation was transgranular through the LPM™ material.

The remainder of the specimens tested at total strain ranges of 0.5% or higher had rougher and more convoluted fracture surfaces. In some cases the fatigue fracture surfaces contained steps, indicating that two dominant cracks had joined at some time during the growth process. As shown in Figure 8, the rough fracture surfaces at the higher strain ranges were associated with a change to an intergranular mode of Stage II crack propagation. This intergranular propagation was associated with fracturing of the Cr_3B_3 precipitates. Note that this change also occurred at a strain level corresponding to the divergence in cycles to crack initiation for cast Inconel 738 vs. the LPM™ hybrid overlay specimens in the continuous cycling tests (Figure 2).

Samples B3 and B4 (outliers) had larger isolated pores which were not typical of the rest of the specimens. Upon examination of the fracture surfaces, one of these samples was found to contain a 0.40 mm x 0.50 mm pore (Figure 8), and the other contained a 0.40 mm x 0.50 mm cluster of interconnected porosity, each of which acted as the primary crack initiation sites. Both features were surface connected. The porosity in the remainder of the samples, as determined by fractography, metallography, FPI and radiographic inspections was 0.25 mm or less in diameter and randomly distributed.

Discussion

Compared to cast Inconel 738, the LCF properties of the LPM™ hybrid overlay samples were considered to be very good, not only in the context of a powder metallurgy (P/M) repair material, but also in view of the difficulties associated with sample preparation and the effects which this had on the base alloy microstructure.

It is well established that the LCF capability of P/M superalloys is largely controlled by the presence of defects such as pores, inclusions and contaminated prior particle boundaries [10-12].

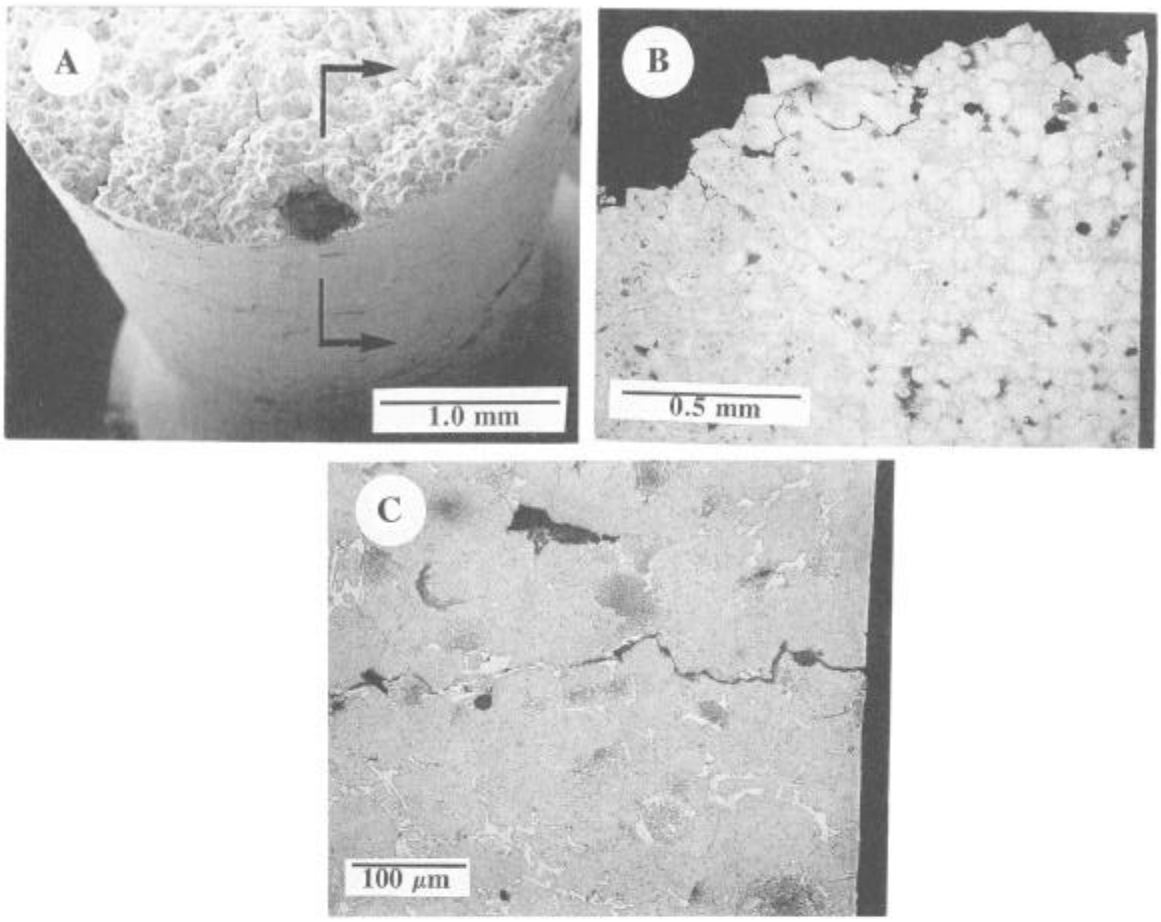

Figure 8. SEM fractograph (A) and optical micrographs of the fatigue fracture surface on sample B3 ($\Delta\epsilon_T$ = 0.6%, N_f = 42 cy., trapezoidal wave form). The arrows in (A) indicate the orientation of the polished cross section. This sample was one of the outliers with an initiation site corresponding to the 0.40 mm x 0.50 mm pore just beneath the surface of the uniform section. This sample is representative of those tested at $\Delta\epsilon_T \geq 0.5\%$ which had rough fracture surfaces and intergranular crack propagation.

LPM™ contains a random distribution of porosity and the dominant fatigue cracks in all tests initiated at the largest near-surface pores. As the total strain range increased, a larger number of pores were capable of initiating fatigue cracks. This behaviour is similar to the observations of Miner and Gayda [10] and Hyzak and Bernstein [11] on P/M René 95. The former authors also noted that the size of the defects initiating failure increased with decreasing total strain range.

Nevertheless, randomly distributed, spherical porosity of approximately 0.25 mm or less in diameter does not appear to have a limiting influence on the LCF lives of the LPM™ repair material. In the low strain range ($\Delta\epsilon_T < 0.5\%$), the LCF lives of the hybrid LPM™ specimens were approximately equal to those of cast Inconel 738, crack propagation was transgranular and was not associated with any specific microstructural feature in the LPM™ material. Based on similarity in fatigue lives, crack propagation rates in LPM™ vs. cast Inconel 738 may be comparable in this strain range. At the higher strain ranges ($\Delta\epsilon_T \geq 0.5\%$), the fatigue lives of the LPM™ hybrid overlay samples were about half to three-quarters those of cast Inconel 738. It was noted that this was accompanied by a switch to an intergranular mode of crack propagation in the hybrid overlay specimens. Thus, within this pore size range, the principle differences in LCF behaviour between the LPM™ and cast versions of Inconel 738 are believed to be associated with the presence of the grain boundary intermetallic phases in the repair material.

In contrast, the LCF lives of the hybrid overlay specimens with larger near-surface porosity were much shorter. In one case, the pore was roughly spherical, in the other case the defect was an area of interconnected porosity but each had a maximum dimension of approximately 0.5 mm. Qualitatively, the negative effects of larger surface pores on the LCF lives of the hybrid overlay LPM™ specimens are again similar to the behaviour of P/M René 95 alloy [10,12]. At $\Delta\epsilon_T$ = 0.66 %, the cycles to failure in René 95 also decreased by almost an order of magnitude as defect areas increased from approximately 2 x 10^{-3} to 0.25 mm^2. Furthermore, for a given size, internal defects were found to be much less detrimental than those situated at the surface [12].

Experience has shown that the size and volume fraction of porosity within the LPM™ filler material is influenced to a large extent by the form (i.e. slurry, tape or putty) in which it is applied.

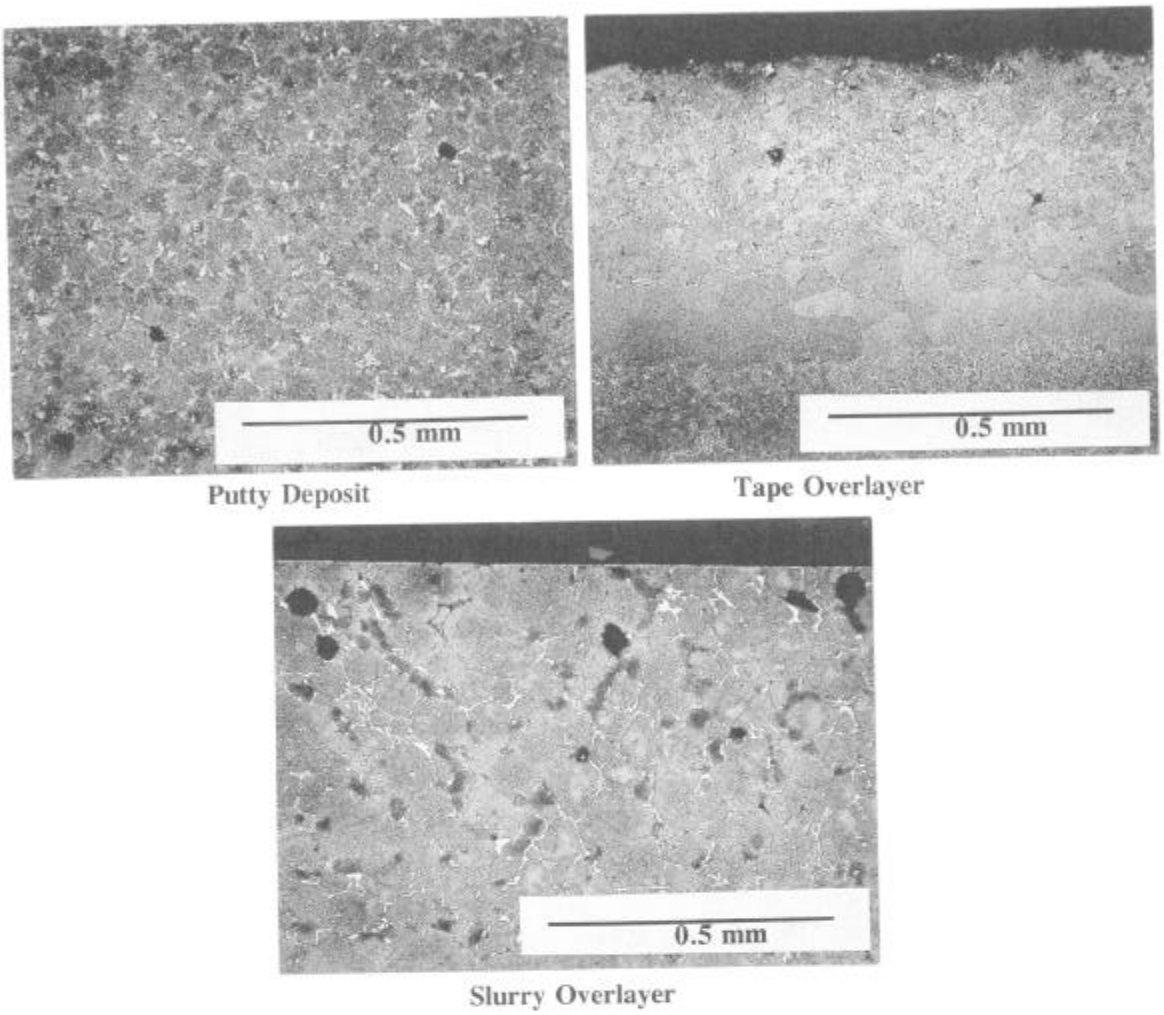

Figure 9. Examples of LPM™ slurry, tape and putty deposits. Note the lower porosity levels in the tape and putty repairs.

Compared to the slurry, the tape and (more recently developed) putty forms of the filler material tend to produce repairs with lower overall porosity. In a typical slurry application, the volume percent of porosity does not exceed four volume percent and is usually less than two percent. In contrast, tape and putty repairs rarely contain more than one percent porosity. In addition, the size distribution of defects within tape and putty repairs is shifted to lower values. Examples of each of these types of LPM™ build-up are shown in Figure 9.

Because of the sensitivity of LCF lives of P/M materials to the size and location of porosity, it will be necessary to specify the appropriate filler material and inspection limits in cases where LPM™ repairs are performed in higher stressed (critical) areas of turbine components. At fatigue sensitive locations, a maximum allowable pore size should be set somewhere between 0.25 to 0.5 mm. Standard penetrant and radiographic techniques are capable of detecting flaws down to about 0.38 mm and should therefore be useful in finding defects of about the critical size. In order to achieve this size limit, it is expected that the tape and putty forms of the LPM™ material will be used in preference to the slurry form.

The results of these laboratory tests are consistent with the results of previously documented field tests on LPM™-repaired Inconel 738 nozzle guide vanes (NGVs)[13]. The NGVs were from an engine used in the propulsion of a hydrofoil. This test environment was considered to be severe, in that the engine experienced approximately one major thermal fatigue cycle (start/stop) per hour of operation. The NGVs were originally removed from service due to extensive thermal fatigue cracking in the outer shrouds and airfoil trailing edge fillet radii. The most severe cracking occurred in the shroud "windows" where at least one 2.5 cm long, axial crack was found between airfoils in each of the components, Figure 9. Following LPM™ wide-gap repair, the NGVs were returned to service alongside new components for an additional 2409 hours. At the following inspection, damage was found to be similar on both the "new" (non-repaired) NGVs and those repaired by LPM™. None of the LPM™-repaired NGVs had re-cracked along the airfoil trailing edges and there was an equal probability of finding a major axial shroud crack in a repaired window or in an adjacent, non-repaired window. Together, the laboratory and field testing have shown that the LPM™ wide-gap method provides a viable solution to many of the problems encountered by existing repair processes.

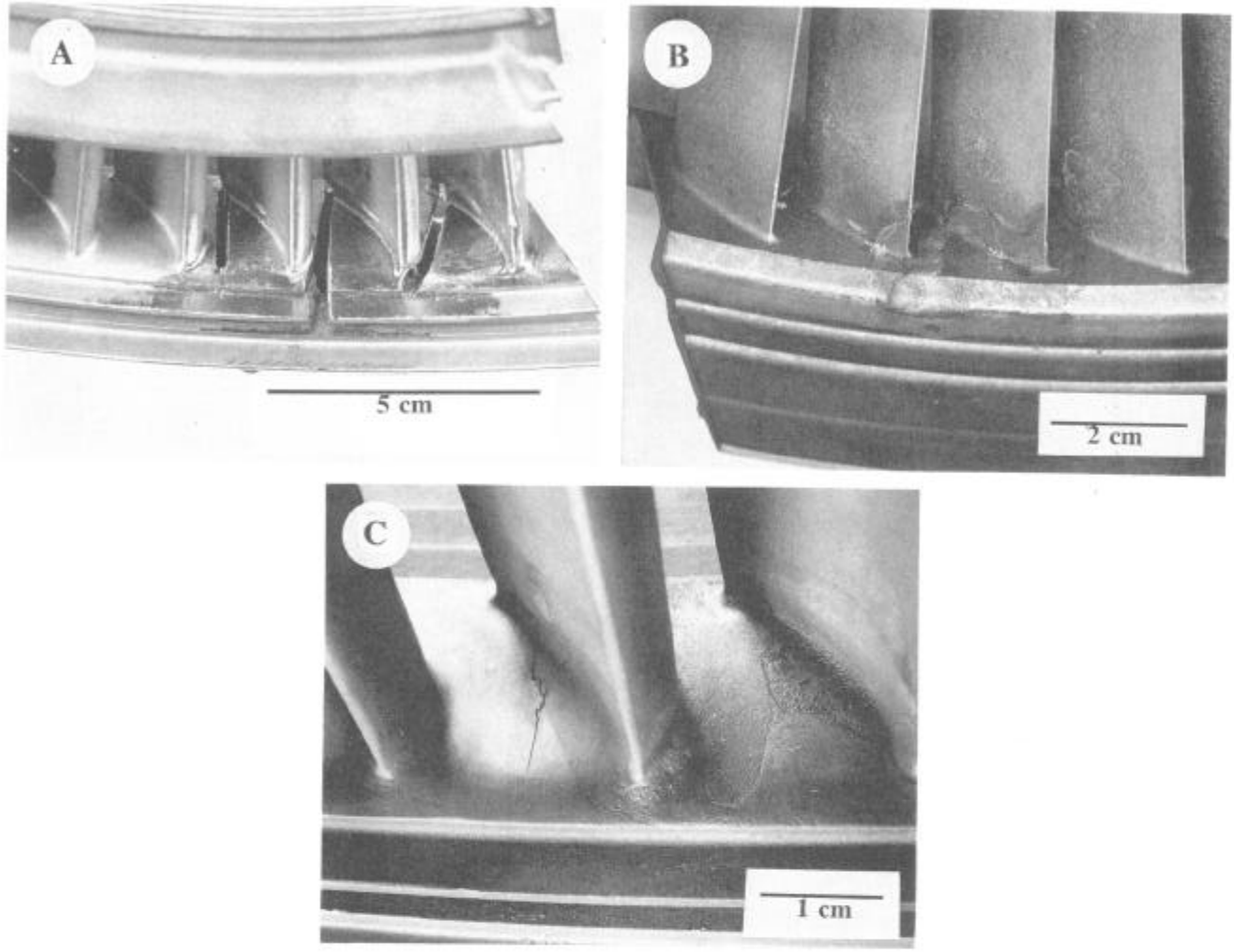

Figure 10 (A) Inconel 738 nozzle guide vane after bench grinding to rout out the crack defects in preparation for LPM™ application. (B) Vane segment after application and heat treatment of Inconel 738 LPM™ repair material. Note also the repaired trailing edge fillet radii. (C) Vane segment after 2409 hours of operation. Recracking was observed in an adjacent window to which LPM™ repair was applied, but not in the LPM™ filler.

Conclusions

1. The low cycle fatigue properties of Inconel 738 LPM™ hybrid overlay specimens were established at 850°C over a total strain range of 0.4 to 0.9 percent in continuous cycling and compressive dwell tests. When near-surface pore dimensions were less than 0.25 mm, the fatigue lives of the repair material were approximately equal to those of cast Inconel 738 at strains below 0.5 percent and one-half to three-fourths those of Inconel 738 at the higher strains.
2. Specimens containing near-surface pores with maximum dimensions of 0.5 mm had much shorter LCF lives. This indicates that, for low cycle fatigue conditions, a maximum allowable pore size should be set somewhere between 0.25 and 0.5 mm. The use of LPM™ in tape and putty form, which have lower overall porosity levels, should help to ensure that this porosity size limit is met.

Acknowledgements

The authors wish to thank the Electric Power Research Institute and co-funding utilities (Anchorage Municipal Light and Power, Duke Power, Florida Power Corp., Nevada Power, Salt River Project and Tri-States Generation and Transmission) for their financial support of this study and permission to publish this data. Dr. Henry Bernstein of the Southwest Research Institute assisted with the planning and analysis of the LCF tests. The many helpful suggestions and comments of Paul Lowden of Liburdi Engineering Limited and Scott Sheirer of Power Tech Associates Inc. are gratefully acknowledged.

References

1. "Gas Turbine Blade Life Assessment and Repair Guide," (Report GS-6544, Research Project 2775-6, EPRI, 1989), pp 7-1 to 7-3.

2. K. Schneider, B. Jahnke, R. Bürgel and J. Ellner, "Experience with Repair of Stationary Gas Turbine Blades - View of a Turbine Manufacturer," Materials Science and Technology, 1 (1985), 613 - 619.

3. P. Brauny, M. Hammerschmidt and M. Malik, "Repair of Air-Cooled Turbine Vanes of High Performance Aircraft Engines - Problems and Experience," *ibid*, 1 (1985), 719 - 727.

4. K. A. Ellison, P. Lowden and J. Liburdi, "Powder Metallurgy Repair of Turbine Components," Journal of Engineering for Gas Turbines and Power, 116 (1994), 237-242.

5. J. Liburdi, K. A. Ellison, J. Chitty and D. Nevin, "Novel Approaches to the Repair of Vane Segments," (Paper No. 93-GT-230 presented at the International Aeroengine Congress and Exposition, Cincinnati, Ohio, 24-27 May 1993).

6. K. A. Ellison, P. Lowden, J. Liburdi and D. Boone, "Repair Joints in Nickel-Based Superalloys with Improved Hot Corrosion Resistance," (Paper No. 93-GT-247 presented at the International Aeroengine Congress and Exposition, Cincinnati, Ohio, 24-27 May 1993).

7. R. Stickler, ed. Summary of the Physical and Mechanical Property Data of the Ni-Base Superalloy IN-738, (University of Vienna, Institute for Physical Chemistry, Materials Science, Report No. 81-UW-COST-B1, 1981).

8. V.S. Ostergren, "A Damage Function and Associated Failure Equations for Predicting Hold Time and Frequency Effects in Elevated Temperature Low Cycle Fatigue", Journal of Testing and Evaluation, 4 (5) (1976), 327-339.

9. F. Gabrielli, M. Marchionni and G. Onofrio, "Time Dependant Effects on High Temperature Low Cycle Fatigue and Fatigue Crack Propagation of Nickel-Base Superalloys", Advances in Fracture Research, (Proceedings of the 7th Conference on Fracture (ICF7), Vol. 2, Houston, Texas, March 1989), 1149-1163.

10. R. V. Miner and J. Gayda, "Effects of Processing and Microstructure on the Fatigue Behaviour of the Nickel-Base Superalloy René 95," International Journal of Fatigue, 6 (3) (1984), 189-193.

11. J. M. Hyzak and I. M. Bernstein, "The Effects of Defects on the Fatigue Crack Initiation Process in Two P/M Superalloys: Part I. Fatigue Origins", Metallurgical Transactions A, 13A (1982), 33-43.

12. D. R. Chang, D. D. Kruger and R. A. Sprague, "Superalloy Powder Processing, Properties and Turbine Disk Application," Superalloys 1984, ed. M. Gell et al. (Warrendale, PA: The Metallurgical Society, 1984), 245-273.

13. K. A. Ellison, "Field Testing of LPM™ Repairs on Allison 501KF Second Stage Vanes," (Report No. 92-6-50A, Liburdi Engineering Limited, 15 July, 1992).